Cement and Concrete Research 40 (2010) 947–955

Contents lists available at ScienceDirect

Cement and Concrete Research

journal homepage: http://ees.elsevier.com/CEMCON/default.asp

Roughness of fracture surfaces and compressive strength of hydrated cement pastes

Tomáš Ficker [a,*], Dalibor Martišek [b], Hamlin M. Jennings [c,d]

[a] Brno University of Technology, Faculty of Civil Engineering, Department of Physics, Veveří 95, 602 00 Brno, Czech Republic
[b] Brno University of Technology, Faculty of Mechanical Engineering, Department of Mathematics, Technická 2, 616 62 Brno, Czech Republic
[c] Northwestern University, Department of Civil and Environmental Engineering, Evanston, Illinois 602 08, USA
[d] Northwestern University, Department of Materials Science and Engineering, Evanston, IL 60208-3109, USA

ARTICLE INFO

Article history:
Received 16 November 2009
Accepted 1 February 2010

Keywords:
Roughness numbers (B)
Fracture surfaces (B)
Cement-based materials (D)
Confocal microscopy (B)
Compressive strength (C)

ABSTRACT

A new type of roughness number Rn_o is formulated as a possible analytical tool for surface studies using confocal microscopy. The formulation accommodates fractal dimension and both of the boundary length scales limiting the fractal region of the fracture surface under investigation. Besides the number Rn_o other roughness characteristics are discussed and their effectiveness in the field of cementitious materials is tested. 3D-surface profile *SP* and surface roughness *SR* parameters designed for surface 3D-analysis were calculated for fracture surfaces of hydrated Portland cement pastes with different values of water-to-cement ratio. The surface profile *SP* parameters monotonically increased with water-to-cement ratio and monotonically decreased with compressive strength. A short discussion of possible reasons for such a behavior is presented.

1. Introduction

Fracture surfaces of cement-based materials have been a focus of interest for many decades. During that time different instrumental techniques have been employed for the surface studies in order to resolve a variety of problems among which the question of the relationship between surface topology and mechanical properties is dominant.

Probably the first application of confocal microscopy in the field of cement-based materials was realized by Lange et al. [1] in 1993. These authors compared roughness numbers (*RN* — see Section 2) of several specimens of hydrated cement pastes and mortars. A great deal of their paper was devoted to the implementation of confocal technique and software processing of confocal optical sections in digital surface topographic maps. Shortly afterwards the same authors presented a more comprehensive paper [2] in which they correlated roughness numbers of fracture surfaces to mechanical parameters such as critical stress intensity factor K_{Ic}, critical effective crack length a_c, compressive strength σ_c, total porosity, and effective pore diameter. The results of this study pointed to a strong correlation between roughness numbers and stress intensity factor K_{Ic} as well as crack length a_c whereas only weak correlation was observed with compressive strength σ_c. Almost no correlation was found for all the other material properties (total porosity and effective pore diameter).

In 1995 Zampini et al. [3] used the confocal microscopic technique to investigate the regions near the interface between cement paste and aggregate within concrete material. The roughness in the proximity of the paste-aggregate interface was found to be higher than that of the paste outside the interface. They repeatedly confirmed a clear correlation between the critical stress intensity factor K_{Ic}, the critical crack extension Δa_c and the roughness of the fracture surfaces of cementitious materials. One year later Lange et al. [4] experimentally and theoretically studied toughening of cement-based matrices reinforced by randomly distributed microfibers and employed confocal microscopy to quantify fracture surfaces of these species. Their work showed that specimens reinforced with microfiber possessed greater crack path tortuousity than the unreinforced specimens. At high magnifications a much higher roughness was observed in the matrix adjacent to fibers than in the matrix without fibers. They concluded by stating that the higher roughness of regions adjacent to fibers indicated an effective crack deflecting caused by the fibers and, as a consequence, stimulated toughening mechanisms in the nearby matrix.

Confocal measurements of roughness were also carried out [5] on oriented Si single crystals in order to explore the relationship between roughness and fracture toughness. It was shown that for brittle fracture with rough surface the fracture toughness is characterized by quantitative surface parameters such as surface roughness and fractal dimension increment. Some other papers [6,7] analyzed the geometry of fracture surfaces of hydrated cement materials by confocal technique and used the geometric parameters as input data for a micromechanical model to predict the increase in toughness due to aggregates.

In all the former papers the authors have used confocal microscopy to determine surface properties (roughness or other geometric characteristics) of fracture specimens in order to correlate these

* Corresponding author. Tel.: +420 541 147 661.
E-mail address: ficker.t@fce.vutbr.cz (T. Ficker).

0008-8846/$ – see front matter © 2010 Elsevier Ltd. All rights reserved.
doi:10.1016/j.cemconres.2010.02.002

properties to some fracture mechanical quantities. In addition to this type of research, there is another research branch [8–10] that employs confocal microscopy for microstructural investigation, especially for pore structure and "Hadley" grains.

The main goal of this paper is to find surface parameters that are sensitive to changes in water-to-cement ratio and compressive strength of cementitious materials and in this way to complement the presently used roughness numbers that are insensitive to these significant material properties.

2. Roughness numbers

Scanning confocal microscopes actually are optical microscopes with a very small depth of field which ensures that the confocal images show only those parts of objects that are very near to the focus plane while other parts, farther from the focal plane, are invisible on the images. Stepping the focus plane through a range of vertical positions provides a series of optical sections from which the software reconstructs a 3D surface digital map (surface relief) as seen in Fig. 1.

So far in the field of fracture mechanics of cementitious materials confocal microscopes have been used to determine roughness numbers *RN* of fracture surfaces. The roughness number has been introduced as the ratio of the area A_s of the fracture surface reconstructed by the confocal technique to the nominal area A_o which is a vertical projection of the fracture surface onto the horizontal *xy*-plane

$$RN = \frac{A_s}{A_o} \geq 1. \tag{1}$$

A good illustration of *RN* offers the so-called "wire" model ("wire" map) of the reconstructed fracture surface presented in Fig. 2. The area A_s can be approximated by the sum of all the surface "wire" cells whereas A_o is the area of the vertical projection of the whole "wire" surface onto the plane *x*,*y*.

Fracture surfaces are often treated as fractals, i.e. their area is calculated as a scale-dependent quantity and follows a scaling relation in which fractal dimension is included. The roughness number *RN* was introduced to quantify an "area gain" of fracture surfaces and as such it should also be a fractal quantity following a scaling relation (scaling with size of cell). This scaling relation should contain the same fractal dimension as the area of the fracture surface. In the following paragraph it is shown that *RN* does not represent a true fractal quantity since its value is calculated outside of the true fractal region. As an alternative to *RN* a new roughness number Rn_o is introduced as a quantity that is calculated within the fractal region and fulfils all the attributes of the true fractal quantity.

Let us suppose that the fracture surface is represented by a confocal image $[R(pixels) \times R(pixels)]$. The area A_s of the surface is then scaled by means of the fractal dimension *D* in the whole length interval $(1, R)$

$$A_s = A_o \cdot \left(\frac{R}{r}\right)^{D-2}, \quad A_o = R^2, \quad 1 \leq r \leq R, \quad RN(r) = \left(\frac{R}{r}\right)^{D-2} \tag{2}$$

where *r* is the characteristic linear size of the "wire" cells covering the surface (Fig. 2). Usually this computational procedure is performed within the pixel space of the digital 3D-image (3D-matrix) in which the *xy*-pixels in the matrix are associated with *z*-coordinates corresponding to the heights of the surface and the "wire" cells assume the form of triangles constructed between pixels. Although in Fig. 2 the wire cells are represented as quadrilaterals, the area of the surface relief is calculated as the sum of the couples of the triangles that form these quadrilaterals. The variable length *r* is also a linear characteristic size of these triangles which are repeatedly enlarged in the procedure to compute the fractal dimension and boundaries of fractal region.

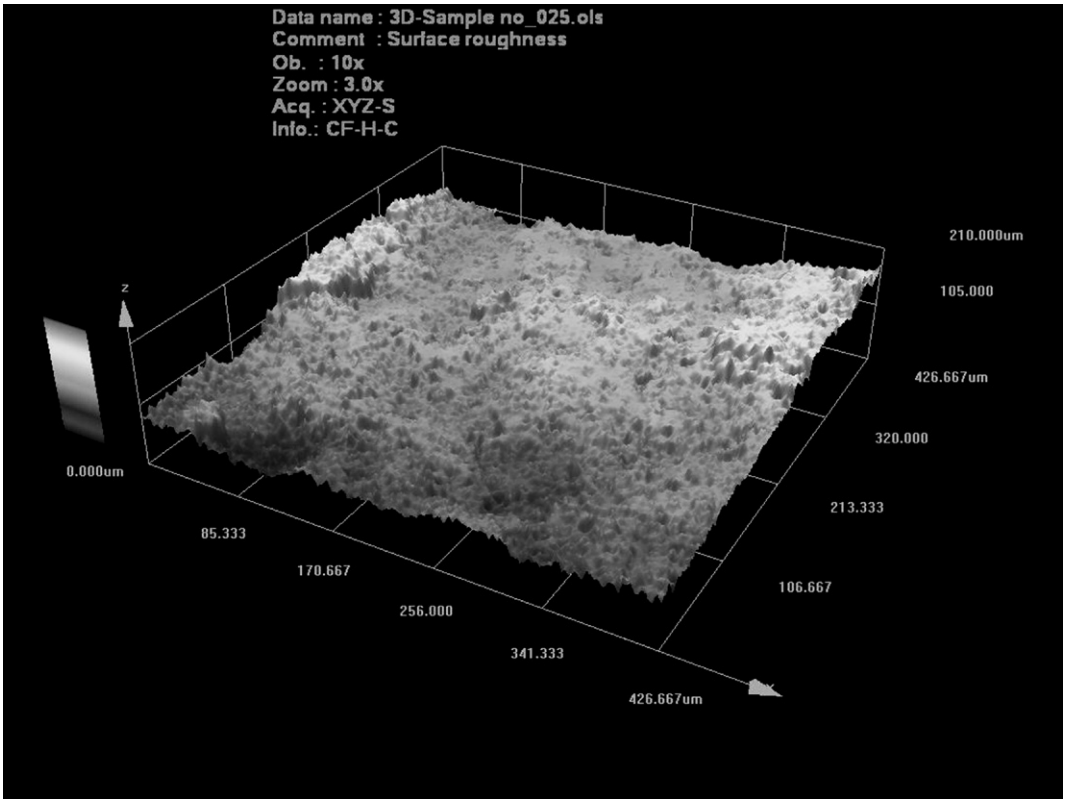

Fig. 1. A digital model of a fracture surface (data from the scanning confocal microscope Olympus Lext 3100, processed by the commercial software Olympus Lext version 6).

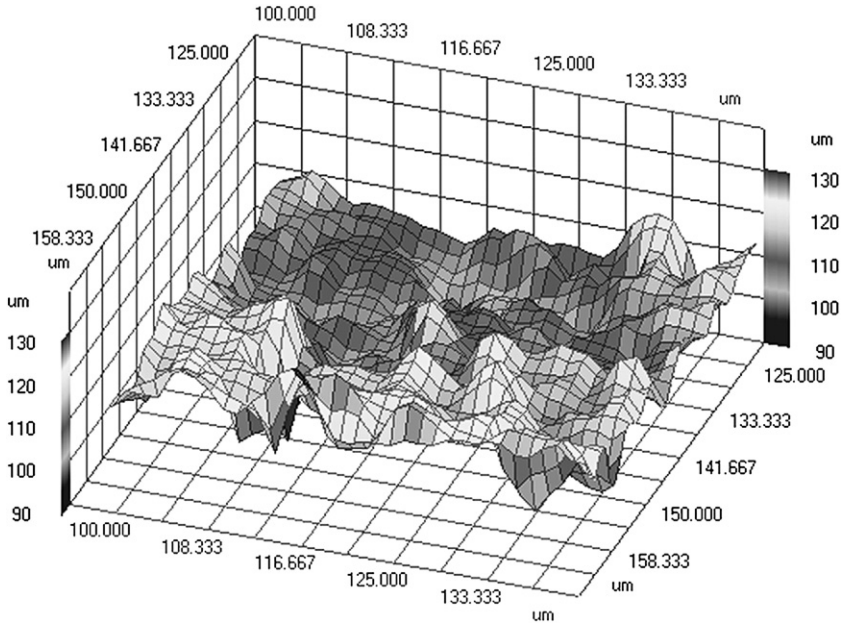

Fig. 2. A wire model of confocal fracture surface (data from Olympus Lext 3100, processed by the software created in our laboratory, author D.M.).

However, due to restricted resolution of confocal microscopes the real fractal region (r_o, R_o) usually is much narrower than the linear size of the confocal picture $R(pixels)$ and, thus, the corresponding scaling relation must reflect this fact

$$S_s = S_o \cdot \left(\frac{R_o}{r}\right)^{D-2}, \quad S_o = R_o^2, \quad r_o \le r < R_o \le R. \tag{3}$$

We suggest a modified roughness number $Rn = S_s/S_o$ that assumes a different value and meaning as compared with *RN*. Being defined as a scaling ratio of the lower (r_o) and the upper (R_o) cutoffs of the fractal region, this is a true *fractal roughness number* without disturbing influences of the two remaining non-fractal regions (1, r_o), (R_o, R)

$$Rn(r) = \left(\frac{R_o}{r}\right)^{D-2}, \quad r_o \le r < R_o \le R. \tag{4}$$

When the original *RN* and *r* are plotted in the log–log system (see Fig. 3), the linear part of the graph will determine the region of fractality (r_o, R_o) and the slope α of this part will determine D

$$D = 2 - \alpha. \tag{5}$$

When r_o, R_o and D are known, the calculation of the *fractal roughness number* Rn_o is a straightforward matter

$$Rn_o = \left(\frac{R_o}{r_o}\right)^{D-2}, \quad r_o \le R_o. \tag{6}$$

Obviously, Eqs. (4) and (6) have no characteristic scale which means that higher resolutions of confocal images will produce still higher values of common roughness numbers $RN(r)$ and $Rn(r)$. But this is not quite the case of the *fractal roughness number* Rn_o. Since the fractal boundaries r_o, R_o are given by a "natural" fracture process itself and not by the measuring procedure, the parameter Rn_o will level off immediately after the resolution of the confocal microscope drops under the length scale r_o and this is surely an appreciable property. The common *RN* number is always outside of the fractal region, as it is calculated for $r = 1$ and r_o is always greater than zero and therefore has nothing in common with the fractal properties of fracture surfaces.

Fig. 3 illustrates differences in determining $RN(r)$ and Rn_o. Using a confocal image 1024 *pixels* × 1024 *pixels*, the data $RN(r)$ were calculated for $r = 1, 2, 3, 4, 5, 6, 7, 8, 10, 12, 15, 19, 25, 40, 63$, and 100 pixels. Within the log–log plot the fractality interval was determined as ($r_o = 5$, $R_o = 19$) along with the dimension $D = 2.305$ and, from these values, the fractal roughness number $Rn_o = 1.503$. In comparison with $RN = RN(1) = 2.450$ the value of the *fractal roughness number* Rn_o is smaller, which might be expected in a majority of cases. Fig. 3 illustrates very clearly that the value of the roughness number *RN* — represented by point A in the graph — is outside of the fractal region (5, 19) and, thus, cannot be considered as a fractal characteristic. This fact disqualifies it from being assumed as a rigorous quantity describing the fractal surface.

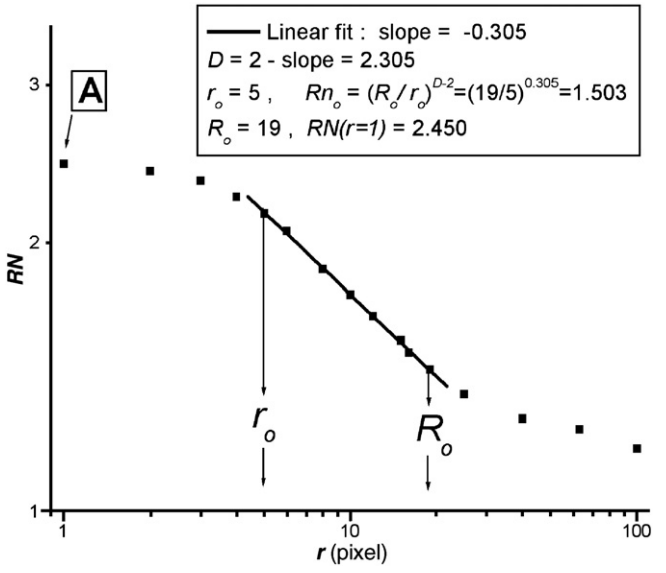

Fig. 3. Determination of fractal roughness number Rn_o from the curve $RN(r)$ plotted in the log–log system. Identification of fractal region (5, 19) in the pixel space.

It is worth noting that the fractal dimension D itself is a scale-independent parameter. However, it is only rarely used in fracture surface analyses even though it has a clear potential for correlation with some mechanical quantities like compressive strength [11–13] or fracture toughness [5]. There are many computational methods [14] for the determination of the fractal dimension, e.g. Minkowski method, box counting method, variation method, slit island method, to mention some of them, but they are often not easy to perform due to their sophisticated algorithm. In addition, their approximative characters are probably the reason why the published values of D show some scatter and sometimes even inconsistency. Calculation of the common roughness number RN is a bit easier than the calculation of D since no region of fractality has to be determined but the roughness number is less general than D because of its non-fractal character. Calculations of fractal roughness numbers Rn_o are as difficult as calculations of fractal dimensions since in both the cases the fractal region must be determined but they both are more general than RN since they have a clearly defined interval of fractality (r_o, R_o) beyond which they do not change their values.

Finally, it is important to note that both the roughness numbers RN and Rno are of the same generic origin, i.e. they represent areal characteristics of fracture surfaces. For this reason Rno may be expected to possess similar correlation properties as RN.

3. Other roughness parameters

There are a number of other roughness parameters [15,16] that are used for the assessment of surface quality in various branches of technology. For instance, mechanical engineers employ a series of surface profile parameters for the evaluation of roughness of metallic surfaces [17]. Many of these concepts may be applied to the analyses of data from confocal microscopy.

The main difference between roughness numbers RN, Rn_o and the roughness parameters employed in mechanical engineering consists in the fact that the mechanical engineers rely more on the selection of local characteristics such as heights of protrusions or depths of depressions, whereas RN, Rn_o accommodate global areal characteristics of surfaces. This situation deserves a detailed explanation.

Let us suppose that a surface can be approximated by an analytical function $z=f(x, y)$ of two variables x, y. The local approach means that local extremes of the surface function $f(x, y)$ are sought, e.g. all local maxima (peaks) $\{z_i^{(\max)}\}$ or all local minima (valleys) $\{z_i^{(\min)}\}$ from which total extremes are deduced, i.e. the total maximum (highest peak)

$$Z_p^{(\max)} = \max\left\{z_i^{(\max)}\right\} \tag{7}$$

or total minimum (deepest valley)

$$Z_v^{(\min)} = \min\left\{z_i^{(\min)}\right\}. \tag{8}$$

Another possibility is to determine an average (mean) value of "pseudo-height" derived from the whole surface function $f(x, y)$

$$H_a = \frac{1}{L\cdot M}\iint_{(LM)} |f(x,y)|dx\,dy \tag{9}$$

or root mean squared "pseudo-height" may be another alternative

$$H_q = \sqrt{\frac{1}{L\cdot M}\iint_{(LM)} [f(x,y)]^2 dx\,dy} \tag{10}$$

where $L\times M$ is the area of vertical projection of the whole surface $f(x, y)$ into the plane xy.

The mentioned four surface characteristics (7)–(10) represent only a small sample of many tens of other similar characteristics that have been introduced [15,16]. They are usually termed as 3D surface characteristics. There are also 2D characteristics that are related to the vertical cross-sectional profiles $z=f(x)_{y=const}$ and $z=f(y)_{x=const}$. The 2D characteristics are commonly used especially in the field of mechanical engineering [17–19] but 3D characteristics are rarely used [20] due to their demand for high-tech devices capable of creating digital maps $f(x, y)$ of solid surfaces. Actually, there are no published applications of 3D surface characteristics to fracture surfaces of cementitious materials. The present paper represents a first attempt to apply this kind of parameters to such surfaces.

It is not easy to foresee the convenience of a 3D parameter for a particular application. Only experimental results can provide a decisive report. For the purpose of examination of fracture surfaces of hydrated Portland cement pastes with different values of water-to-cement ratio three kinds of 3D parameters have been identified as possible candidates that could be sensitive to the differences in w/c ratio. These parameters were designated as SPp, SPa and SPq and are related to the surface function $f(x, y)$ as follows: SPp is identical with $Z_p^{(\max)}$ as given by Eq. (7), SPa and SPq are "pseudo-heights" as given by Eqs. (9) and (10), respectively. They are called 3D surface profile parameters since they refer to the surface profile function $f(x, y)$. Besides these parameters there is a second class of true roughness parameters that are defined in a full analogy to the profile parameters and bear a similar notation — SRp, SRa, SRq. These new roughness parameters are not related to the surface profile function $f(x, y)$ but, instead, they are derived from a modified surfaces roughness function $f_R(x, y)$ which results from that of profile $f(x, y)$ after filtering out the long "wavelengths". Filtering out the long wavelengths from wavy shaped function $f(x, y)$ is rather an individual procedure since a precise criterion for the determination of a critical wavelength has not been defined for this operation. In this paper both the sets of parameters (SPp, SPa, SPq) and (SRp, SRa, SRq) are tested on the hydrated cement paste. A value of 100 pixels was chosen as the critical wavelength for the filtering procedure in the present work.

To explain the filtering procedure in more detail, the scheme in Fig. 4 shows the situation in one dimension, i.e. the profile function $f(x)$ and roughness profile function $f_R(x)$ that was obtained from $f(x)$ after applying the high-pass filter with a critical wavelength λ_c. In our case $\lambda_c=100$ pixels and $L=M=1024$ pixels were used. Such a filtering removes "waves" with wavelength longer than that of critical λ_c and leaves shorter wavelengths untouched. Therefore, the roughness parameters that are derived from the roughness profile $f_R(x)$ are restricted to smaller length scales as compared with profile parameters derived from the initial profile $f(x)$. For such a numerical filtering there are available commercial software filters of various types, e.g. Gaussian filters or wavelet filters which are usually parts of larger

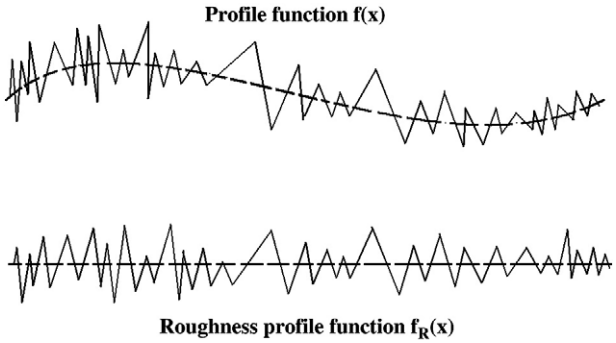

Fig. 4. Scheme illustrating the filtration of profile function $f(x)$ and creation of roughness profile $f_R(x)$.

software packages supplied with measuring devices as in the case of Olympus Lext 3100.

It should be mentioned that both the 3D profile *SP* and roughness *SR* parameters, mentioned above, are also scale-sensitive. Otherwise the values between mutually corresponding *SP* and *SR* could not be different and would attain the same values. Filtering out of longer "wavelengths" from the surface function $f(x, y)$ and receiving of a modified function of roughness $f_R(x, y)$ actually is a transition to a shorter length scale and this makes the values of *SP* and *SR* different. A fracture surface on different length scales shows different roughnesses and this is the reason why the *SP* and *SR* parameters may independently co-exist.

In this study, *RN*, *Rno*, *SP* and *SR* were correlated with *w*/*c* and compressive strength σ_c. The measurements were performed on a series of specimens with different values of *w*/*c*. Since porosity and compressive strength are largely determined by *w*/*c*, this enabled us to develop considerations about the correlation between the parameters *RN*, *Rno*, *SP*, *SR* and porosity without measuring directly the porosity of the material. Nevertheless, compressive strength was measured directly to plot exact graphs $SP(\sigma_c)$ and $SR(\sigma_c)$. The main goal of the paper is to find surface parameters that show a clear dependence on *w*/*c* ratio since such parameters might report on the *w*/*c* values perhaps many years after the initial preparation of the material, which could be a valuable information in the case of a construction failure.

4. Experimental details

Forty-eight samples (2 cm × 2 cm × 10 cm) of hydrated ordinary Portland cement paste of various water-to-cement ratios *w*/*c* (0.4, 0.6, 0.8, and 1.0) were prepared (12 samples per each value of *w*/*c*). The samples were rotated during hydration to achieve their better homogeneity. After 28 days of hydration the samples were fractured in three-point bendings and the fracture surfaces were immediately used for further microscopic analyses. Using a confocal microscope, Olympus Lext 3100, approximately 80 image sections were obtained for the samples starting from the very bottom of the surface depressions to the very top of the surface protrusions with the step of 4 μm. The investigated area $L \times M = 1280\ \mu m \times 1280\ \mu m$ (1024 pixels × 1024 pixels) was chosen in five different places of each fracture surface (in the center and in the four positions near the corners of the rectangular area), i.e. each plotted point of the graphs of roughness numbers and parameters corresponds to an average composed of 60 measurements (12 samples × 5 surface measurements). The microscopic sections served as a basis for digital reconstructions of fractal self-affine surfaces (Fig. 1). These 240 fracture surfaces in digital forms were then subjected to profile and roughness surface analyses using the commercial software of the confocal microscope Olympus Lext 3100.

The main contribution to porosity manifested in our digital images results from the capillary pores whose maximum size depends on factors such as type of material, stage of hydration, *w*/*c*, etc., with the maximum size of such pores reaching a value of several micrometers. Owing to the resolution 1.25 μm per pixel only the largest capillary pores contribute to the detected pore structure on the fracture surfaces. Since the whole field of view is approximately 1 mm, the larger air voids (>1 mm), which usually represent a small volume fraction (less than 3%), do not play any important role. Capillary porosity determines the compressive strength of cement paste, so it is natural to expect that there could be some correlation between the compressive strength, capillary porosity (governed by water-to-cement ratio) and surface parameters (*SP* and *SR*).

As mentioned in the preceding paragraphs, the samples were fractured so that two specimens approximately 5 cm long were obtained from each original sample. One specimen was used for microscopic analysis, as described above, whereas the second one was utilized for the determination of the compressive strength σ_c. Before compressive tests, the 48 specimens were cut to obtain 48 small cubes with the edge of 2 cm. The surfaces of the cubes were perfectly processed to remove corrugations and to create a good interface between the specimens and the plates of the hydraulic press. The gradually increasing compressive stress (0.04 MPa/s) acted on the cubes up to their breakdown.

5. Results and discussion

This study investigates the relationship between surface geometrical characteristics (*RN*, Rn_o, *SP*, and *SR*) and two material parameters (*w*/*c* and σ_c) of hydrated cement pastes. Since the compressive strength σ_c is one of the applied parameters, it was necessary to measure it along with all the investigated quantities. Its behavior σ_c (*w*/*c*), shown in Fig. 5, follows a recognized relationship [21,22] between compressive strength and *w*/*c* which indicates the proper preparation of all the specimens used. The statistical inaccuracies related to the values of σ_c are less than 10% (relative probability inaccuracy).

Figs. 6 and 7 show dependencies $RN(w/c)$, $Rn_o(w/c)$ and $RN(\sigma_c)$, $Rn_o(\sigma_c)$, respectively. The shapes of their graphs are very similar. This supports the assumption that *RN* and Rn_o are of the same generic origin that is based on the areal properties of fracture surfaces. All the graphs manifest the peak at $w/c = 0.6$ ($\sigma_c \approx 25$ MPa). A striking feature of all these graphs is their partly increasing and partly decreasing behavior. Both the parameters *RN* and Rn_o characterize surface irregularity of fracture surfaces and this irregularity increases with increasing *w*/*c* (increasing porosity due to increasing *w*/*c* makes fracture surfaces more rugged) but the graphs $RN(w/c)$ and $Rn_o(w/c)$ show a decrease for $w/c > 0.6$ instead of the expected increase. This evokes the idea that the configuration of the measured points may represent a pattern of uncorrelated points rather than a regular functional dependence. Such an idea is supported by the results of Lange et al. [2]. These authors showed that *RN* versus porosity with cement-based materials are fully uncorrelated quantities (see their Fig. 13 in [2]). Similar situation was reported for *RN* versus σ_c

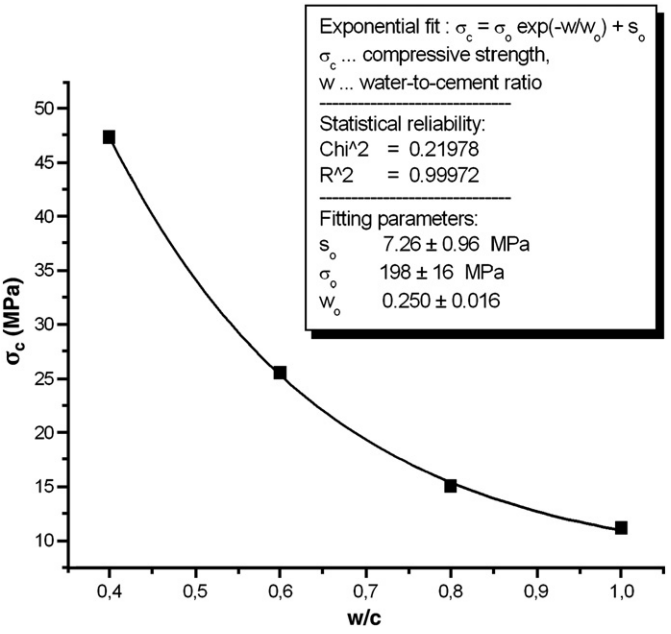

Fig. 5. Curve of compressive strength showing exponential decrease with water-to-cement ratio. Samples with higher *w*/*c* do not perturb the exponential behavior which indicates their acceptable structural consistency.

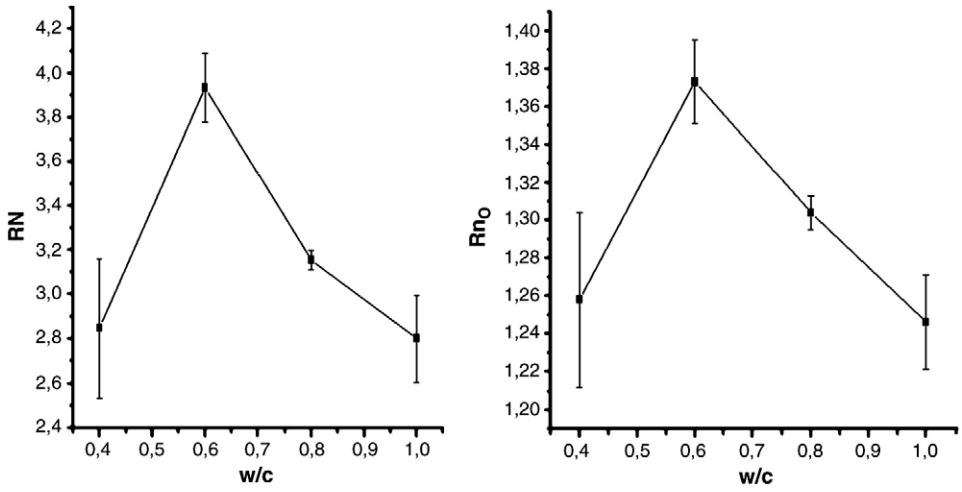

Fig. 6. Dependence of roughness numbers *RN* and Rn_o on water-to-cement ratio.

(Fig. 15 in [2]). Nevertheless, to draw a definitive conclusion, it would be desirable to have more experimental points, at least for $w/c = 0.5$, 0.7 and 0.9. This should be a task for further research.

Fig. 8 contains a collection of six graphs illustrating dependences of profile *SP* and roughness *SR* parameters on *w/c*. Almost all of these graphs show increasing values with *w/c*, i.e. the cases when the fracture surfaces of higher *w/c* ratio become more irregular and rougher. The higher irregularities (higher *SP*) and higher roughening (higher *SR*) of these surfaces correspond to higher porosity of the samples with increasing *w/c*. The idea that porosity considerably influences the height irregularities of fracture surfaces is supported by the experimental findings of Ponson et al. [23,24]. Ponson's graph [23] reproduced in Fig. 9 documents this fact very clearly. This figure shows vertical profiles of fracture surfaces in dependence on porosity. The height irregularity of surfaces evidently increases with increasing porosity.

Another collection of six graphs $SP(\sigma_c)$, $SR(\sigma_c)$ in Fig. 10 provides a direct insight into the behavior of profile and roughness parameters for varying compressive strengths. They unambiguously show decreasing functions especially in the case of $SP(\sigma_c)$. The conclusion that stronger hydrated Portland cement pastes have smoother fracture surfaces is not surprising since finer and more compact structures are known to guarantee better compressive strength in comparison to their counterparts with high porosity. And again, the assumption of a close connection of profile and roughness parameters to porosity facilitates the explanation of the existing dependency between surface quality and mechanical strength.

Comparing the graphs in both Figs. 8 and 10, we note that the *SP* parameters, in contrast to *SR*, have a smoother monotonic behavior without any "waves or humps" (that could cause ambiguous reading). Thus *SP* may be convenient for monitoring changes in *w/c* ratio. The statistical uncertainties with *SP* and *SR* are indicated by error bars similarly as in the preceding graphs. Due to high surface stochasticity of this material, it might be desirable still more to increase the number of specimens and surface measurements to decrease the statistical uncertainty of the results.

Let us discuss the shape of the measured $SP(w/c)$ dependences in Fig. 8. The graphs show two characteristic regions: (i) a region $w/c \in (0.4, 0.8)$ of slightly increasing roughness, (ii) a region $w/c > 0.8$ of abruptly increasing roughness. A similar phenomenon was described by Ponson [23]. He studied the roughness of fracture surfaces with glass ceramics made of small glass beads sintered in bulk with the porosity that could be varied in a certain interval up to ~30%. He found that at small porosities the roughness of fracture surfaces varied only

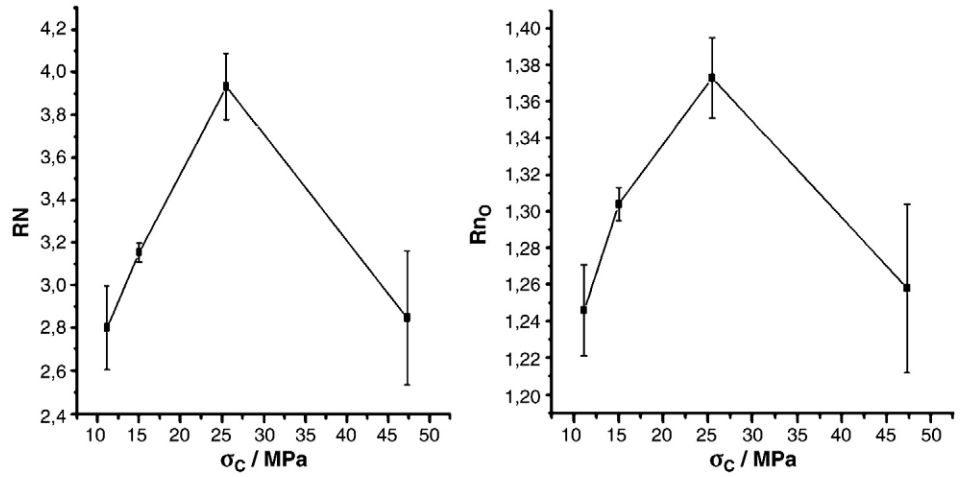

Fig. 7. Dependence of roughness numbers *RN* and Rn_o on compressive strength.

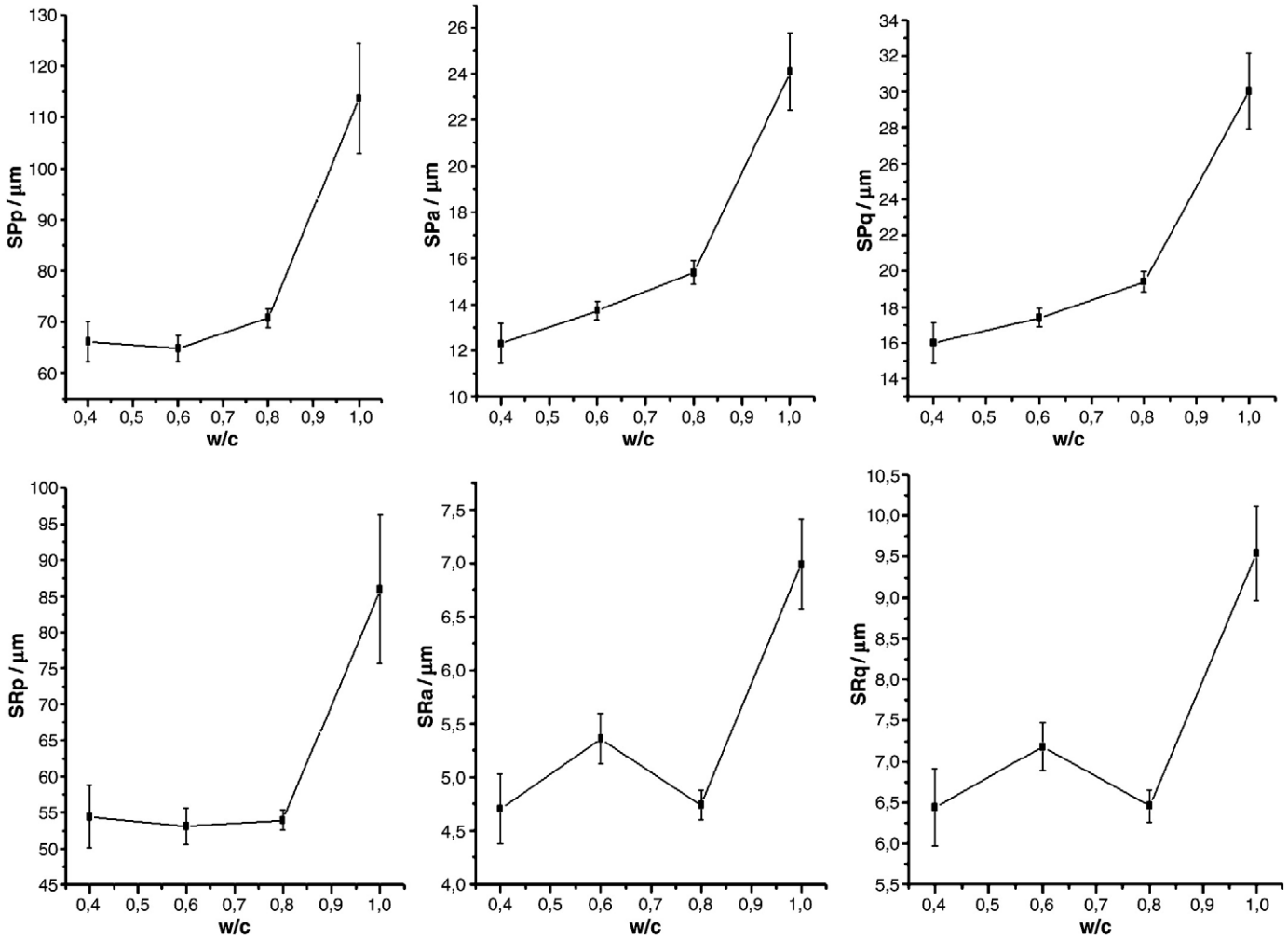

Fig. 8. Dependence of profile *SP* and roughness *SR* parameters on water-to-cement ratio. Monotonically increasing functional behavior found with parameters *SP*.

moderately in a quasi-linear fashion (region of "transgranular fracture" [23]) whereas at higher porosities he observed a fast increase of roughness (region of "intergranular fracture" [23]). Although the glass ceramics and cement-based materials are rather different materials they seem to show similar fracture properties.

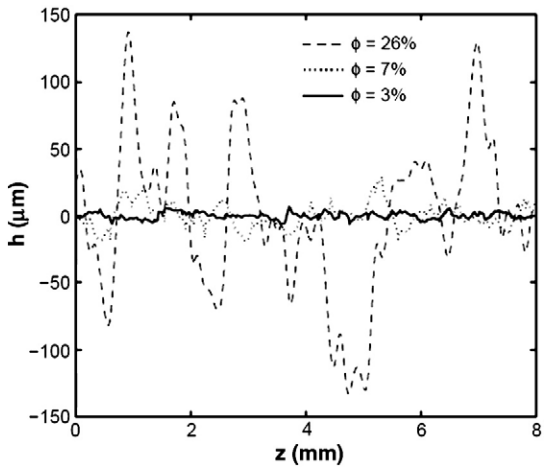

Fig. 9. Vertical profiles of fracture surfaces in dependence on porosity. Reproduced from [23] - courtesy of L. Ponson.

As far as the shape of the measured $SR(w/c)$ and $SR(\sigma_c)$ dependencies is concerned, it is possible to notice smaller peaks at $w/c = 0.6$ and $\sigma_c \approx 25$ MPa (Figs. 8, 10). Since their localizations are identical with the peaks in the graphs of *RN* and Rn_o shown in Figs. 6 and 7, they might be of the same origin. Assuming the hypothesis of the uncorrelated scatter of measured points, the question arises why the points in the graphs $SR(w/c)$ and $SR(\sigma_c)$ should be less correlated as compared with those of the graphs $SP(w/c)$ and $SP(\sigma_c)$. To answer the question, it is necessary to realize the following facts: The parameters *SPa* and *SPq* were determined as average values by integration over all the field of view (1024 pixels × 1024 pixels). Due to the integration of the surface profile extending over the whole field of view, they "absorbed" surface properties on all length scales given by the interval (1, 1024) pixels. It means that *SPa* and *SPq* are global characteristics bearing information of all length scales. The parameters *SPa* and *SRq* are also global characteristics (integration over 1024 pixels × 1024 pixels) but this integration was performed using the filtered surface profile, i.e. the so-called roughness profile $f_R(x, y)$ with the limiting length scale $\lambda_c = 100$ pixels. Such a filtered profile bears surface information only within restricted length scales given by (1, 100) pixels which inevitably has caused a loss of an essential part of surface height characteristics. For this reason the corresponding graphs of all the *SR* parameters suffer from a weaker relationship to overall surface properties governed by the initial ratio w/c. Thus, they show a weaker correlation to this ratio and, as a consequence, the values of *SR* may form a partly uncorrelated scatter

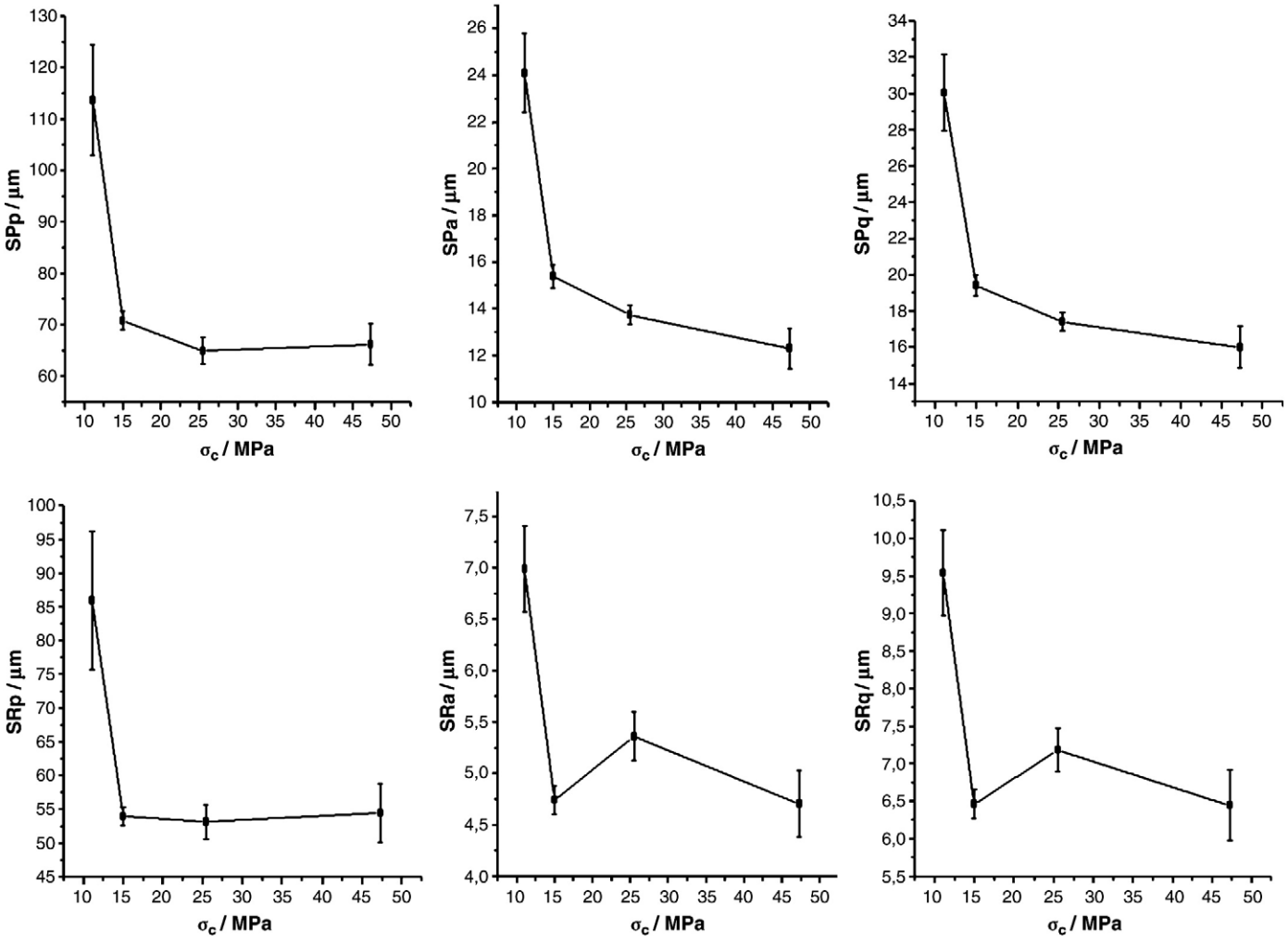

Fig. 10. Dependence of profile *SP* and roughness *SR* parameters on compressive strength. Monotonically decreasing functional behavior found with parameters *SP*.

of graphical points. Extending this hypothesis further to the *RN* and Rn_o numbers, it is convenient to notice their extremely narrow length scales. The length scale of Rn_o was about (5, 19) pixels whereas that of *RN* only 1 pixel. This might explain why these parameters may correlate so weakly to w/c and σ_c. Global properties and complete length scales seem to be important for strong correlation effects.

So far the parameters *SPp* and *SRp* have not been mentioned. They are high localized parameters (point-like characteristics) since they represent the total maxima of the profile $f(x, y)$ and roughness $f_R(x, y)$ functions and as such they completely lose the overall surface characteristics granted by the value of w/c. Their reliability and a stage of correlation, as compared with *SPa* and *SPq*, may be lower.

The main difference between the parameters *SP*/*SR* and the numbers RN/Rn_o consists in the fact that *RN* and Rn_o numbers provide information on surface area (areal properties) but no information on height differences of surface profiles whereas the parameters *SP* and *SR* offer no information on areal properties but provide direct information on the overall height characteristics of fracture surfaces. Since the ratio w/c influences more height differences than the area differences of the fracture surfaces of porous materials, it is the RN/Rn_o numbers that may show almost no correlation to w/c or σ_c. This is probably the decisive factor distinguishing the correlation properties of *SP*/*SR* and RN/Rn_o.

The reasons why profile parameters *SP* correlate with porosity-dependent mechanical quantities, as illustrated in Fig. 10, whereas roughness numbers *RN* correlate with energy-dependent quantities like toughness [2–4] but not with porosity [2], deserve a further discussion. When a crack spreads through a material, two new surfaces of equal areas are created. The corresponding surface energy increases due to its proportionality to growing areas. The greater the roughness of the newly created surfaces, the greater the area and the higher the surface energy. This naturally calls for a larger demand for fracture energy. Therefore, the fracture energy and its related mechanical quantities like toughness become dependent on surface-area changes. Since the roughness number, *RN*, quantifies the area increase, it correlates to quantities such as fracture energy, toughness, etc. It is the areal sensitivity that makes the roughness number *RN* correlate to energy-based mechanical quantities.

During fracture, not only area is extended but also height differentiation takes place. It is the pore network that contributes significantly to this height differentiation. Let us recall that cement pastes of a higher water-to-cement ratio possess higher capillary porosity. The hydrated pastes of Portland cements with $w/c \approx 0.4$ contain about 30% of pores and the porosity increases [22] with increasing values of w/c. In addition, the higher the w/c, the greater the volume fraction of coarse capillary pores of a sample at any given time of their hydration [25]. Coarser pores give rise to larger depressions and edges on the fracture surfaces of porous materials and this explains why the values of profile and roughness parameters are larger with materials possessing higher w/c ratios. Profiles *SP* and

roughness *SR* surface parameters quantify height differences and, for this property, they are associated with those mechanical quantities that are dependent on pores and porosity. A particular example is the found correlation between compressive strength and the profile surface parameters *SP*. All this provides an explanation why the roughness numbers *RN* are correlated to toughness [2–4] and not to porosity [2] and why the profile surface parameters *SP* show close connections with those mechanical quantities that are dependent on porosity and water-to-cement ratio.

6. Conclusion

In addition to the common roughness numbers *RN*, there is a newly defined number called fractal roughness number Rn_o. This parameter is scale-dependent only within the region of fractality of the fracture surface under investigation.

The profile *SP* parameters investigated in this paper have shown a close correlation to water-to-cement ratio and, as a consequence, to compressive strength. Their dependences on water-to-cement ratio have appeared to be increasing functions $SP(w/c)$ whereas for compressive strength they have shown an opposite trend.

The discussion on sensitivity of the numbers *RN*, Rn_o and the parameters *SP*, *SR* has indicated that the former two might be more convenient for correlation to energy-based mechanical quantities whereas the latter two to those of porosity-dependent.

The *SP* and *SR* parameters of 3D-analysis are not frequently employed due to their higher demands for high-tech experimental background. In the field of cementitious materials they are applied here for the first time.

When comparing capability of *SP* and *SR* parameters of monitoring changes in water-to-cement ratio, the parameters *SP* seem to be more convenient for this purpose since they show a higher level of correlation to this ratio and, in addition, their graphs are fully monotonic in all their extents. One of the possible hypotheses why *SR* parameters are not fully monotonic might be the fact that these parameters are determined on the smaller length scales which reduce information on the overall height differences of surfaces. However, this phenomenon would deserve more research. It seems that the *SP* parameters could become a good complement to the roughness numbers *RN* and Rn_o that show sensitivity to energy-based quantities whereas *SP* to porosity, compressive strength and w/c ratios.

The 3D surface profile parameters *SPa* and *SPq* seem to be promising candidates for the evaluation of the initial water-to-cement ratio of cementitious materials. For the verification of their behavior during material ageing it is necessary to perform further research to prove their reliability and stability within a long time period.

Acknowledgement

This work was supported by the Ministry of the Czech Republic under contract no. ME 09046 (Kontakt).

References

[1] D.A. Lange, H.M. Jennings, S.P. Shah, Analysis of surface-roughness using confocal microscopy, J. Mater. Sci. 28 (14) (1993) 3879–3884.
[2] D.A. Lange, H.M. Jennings, S.P. Shah, Relationship between fracture surface roughness and fracture behavior of cement paste and mortar, J. Am. Ceram. Soc. 76 (3) (1993) 589–597.
[3] D. Zampini, H.M. Jennings, S.P. Shah, Characterization of the paste-aggregate interfacial transition zone surface-roughness and its relationship to the fracture-toughness of concrete, J. Mater. Sci. 30 (12) (1995) 3149–3154.
[4] D.A. Lange, C. Quyang, S.P. Shah, Behavior of cement-based matrices reinforced by randomly dispersed microfibers, Adv. Cem. Based Mater. 3 (1) (1996) 20–30.
[5] Y.B. Xin, K.J. Hsia, D.A. Lange, Quantitative characterization of the fracture surface of Si single crystals by confocal microscopy, J. Am. Ceram. Soc. 78 (12) (1995) 3201–3208.
[6] A.B. Abell, D.A. Lange, Fracture mechanics modeling using images of fracture surfaces, Int. J. Solids Structures 35 (31–32) (1997) 4025–4034.
[7] A.B. Nichols, D.A. Lange, 3D surface image analysis for fracture modeling of cement-based materials, Cem. Concr. Res. 36 (2006) 1098–1107.
[8] K.E. Kurtis, N.H. El-Ashkar, C.L. Collins, N.N. Naik, Examining cement-based materials by laser scanning confocal microscopy, Cem. Concr. Compos. 25 (2003) 695–701.
[9] M.K. Head, N.R. Buenfeld, Confocal imaging of porosity in hardened concrete, Cem. Concr. Res. 36 (2006) 896–911.
[10] M.K. Head, N.R. Buenfeld, Confocal imaging of porosity in hardened concrete, Cem. Concr. Res. 36 (2006) 1483–1489.
[11] T. Ficker, Fractal strength of cement gels and universal dimension of fracture surfaces, Theor. Appl. Fract. Mech. 50 (5) (2005) 167–171.
[12] T. Ficker, A. Len, R. Chmelik, L. Lovicar, D. Martisek, P. Nemec, Fracture surfaces of porous materials, Europhys. Lett. 80 (6) (2007) 1600–1604.
[13] T. Ficker, Fractal dimensions of fracture surfaces, J. Eng. Mech. (in print).
[14] E. Charkaluk, M. Bigerelle, A. Iost, Fractals and fracture, Eng. Fract. Mech. 61 (1998) 119–139.
[15] Standard ISO 25 178: Geometric Product Specifications (GPS) — Surface texture: Areal (International Organisation for Standardisation, Technical Committee TC 213).
[16] Image Metrology A/S: image processing software for microscopy. Reference guide: http://www.imagemet.com/WebHelp/spip.htm#roughness_parameters.htm.
[17] Marks' Standard Handbook for Mechanical Engineers, section 13.5 "Surface texture designation, production, and control" by T. W. Wolf (McGraw-Hill, New York, 2007–11th edition).
[18] Y.S. Choi, H.R. Pichler, A.D. Rollett, Introduction and application of modified surface roughness parameters based on the topographical distributions of peaks and valleys, Mater. Charact. 58 (10) (2007) 901–908.
[19] M. Bigerelle, D. Najjar, A. Lost, Relevance of roughness parameters for describing and modeling machined surfaces, J. Mater. Sci. 38 (11) (2003) 2525–2536.
[20] H. Ramasawny, L. Bluntc, K.P. Rajurkar, Investigation of the relationship between the white layer thickness and 3D surfaces texture parameters in the die sinking EDM process, Precis. Eng. 29 (4) (2005) 479–490.
[21] P.K. Mehta, P.J.M. Monteiro, Concrete, Microstructure, Properties and Materials, third editionMcGraw-Hill, New York, 2006.
[22] W. Czernin, Cement Chemistry and Physics for Civil Engineers, Bauverlag GMBH, Wiesbaden, 1980.
[23] L. Ponson, Crack propagation in disordered Materials; How to decipher fracture surfaces (Ph.D. Thesis, Univ. Paris., 2006) (http://pastel.paristech.org/2920/?).
[24] L. Ponson, H. Auradou, M. Pessel, V. Lazarus, J.P. Hulin, Failure mechanisms and surface roughness statistics of fractured Fontainebleau sandstone, Phys. Rev. E 76 (2007) 036108/1–036108/7.
[25] S. Igarashi, M. Kawamura, A. Watanabe, Analysis of cement pastes and mortars by a combination of back scatter-based SEM image analysis and calculations based on the Powers model, Cem. Concr. Compos. 26 (2004) 977–985.